HHS Public Access

Author manuscript

Neuroscience. Author manuscript; available in PMC 2018 April 07.

Published in final edited form as:

Neuroscience. 2017 April 07; 347: 123–133. doi:10.1016/j.neuroscience.2017.02.006.

Klotho regulates CA1 hippocampal synaptic plasticity

Qin Li[1], **Hai T. Vo**[1], **Jing Wang**[1], **Stephanie Fox-Quick**[1], **Lynn E. Dobrunz**[1], and **Gwendalyn D. King**[1,*]

[1]Department of Neurobiology, University of Alabama at Birmingham, Birmingham AL 35294 USA

Abstract

Global klotho overexpression extends lifespan while global klotho-deficiency shortens it. As well, klotho protein manipulations inversely regulate cognitive function. Mice without klotho develop rapid onset cognitive impairment before they are 2 months old. Meanwhile, adult mice overexpressing klotho show enhanced cognitive function, particularly in hippocampal-dependent tasks. The cognitive enhancing effects of klotho extend to humans with a klotho polymorphism that increases circulating klotho and executive function. To affect cognitive function, klotho could act in or on the synapse to modulate synaptic transmission or plasticity. However, it is not yet known if klotho is located at synapses, and little is known about its effects on synaptic function. To test this, we fractionated hippocampi and detected klotho expression in both pre and post-synaptic compartments. We find that loss of klotho enhances both pre and post-synaptic measures of CA1 hippocampal synaptic plasticity at 5 weeks of age. However, a rapid loss of synaptic enhancement occurs such that by 7 weeks, when mice are cognitively impaired, there is no difference from wild-type controls. Klotho overexpressing mice show no early life effects on synaptic plasticity, but decreased CA1 hippocampal long-term potentiation was measured at 6 months of age. Together these data suggest that klotho affects cognition, at least in part, by regulating hippocampal synaptic plasticity.

Keywords

Paired-pulse facilitation; long-term potentiation; brain aging; synaptic plasticity

Introduction

The klotho (KL) protein was originally characterized for its lifespan effects (Kuro-o et al., 1997, Kurosu et al., 2005, Dubal et al., 2014). Overexpression of KL is sufficient to extend mouse lifespan (Kurosu et al., 2005, Dubal et al., 2014). In contrast, KL-deficiency shortens mouse lifespan to ~8 weeks by disrupting phosphate homeostasis (Kuro-o et al., 1997). Increasing evidence implicates a brain-specific function for KL. Short lived KL-deficient

*Corresponding author: Gwendalyn D. King, Ph.D. Department of Neurobiology, University of Alabama at Birmingham, 1825 University Blvd, Shelby 913, Birmingham, AL 35294, 205-996-6247 – phone, 205-934-6571 - fax, gdking@uab.edu.

(KO) mice rapidly develop cognitive impairment between the 5th and 7th week of life (Nagai et al., 2003). Meanwhile long-lived KL overexpressing (OE) mice show increased cognitive function after ~6 months of age (Dubal et al., 2014). As well, KL overexpression is sufficient to protect against the development of Alzheimer's disease-like cognitive and synaptic impairment (Dubal et al., 2015) and may be neuroprotective (Zeldich et al., 2014). Cognitive impacts of KL extend to humans, as those carrying the functional KL-VS polymorphism have increased circulating KL (Arking et al., 2002), larger prefrontal cortical volume, and enhanced cognitive function (Dubal et al., 2014, Yokoyama et al., 2015).

The profound and inverse effects of KL on cognition are not easily explained by the data collected to date which broadly characterize the KO and OE brain. KO brains show slightly increased levels of apoptotic (Shiozaki et al., 2008) and oxidative stress (Nagai et al., 2003) proteins, mild decreases of some synaptic proteins (Shiozaki et al., 2008), a slight stochastic increase in neuron death (Nagai et al., 2003), and loss of some myelinated fibers and oligodendrocytes (Chen et al., 2013). Although OE mouse brains show no cellular changes, neurons are more resistant to oxidative stress (Brobey et al., 2015) and hippocampal NMDA GluN2B receptor subunit expression is upregulated (Dubal et al., 2014). At the level of synaptic function, long-term potentiation (LTP) of KO CA1 neurons is mildly decreased but only when lightly stimulated by a single theta burst (Park et al., 2013). Meanwhile, adult OE hippocampal dentate gyrus recordings show increased LTP (Dubal et al., 2014).

KL is expressed by both neurons and the choroid plexus, the endothelial cells that form the blood:cerebrospinal fluid barrier and generate cerebrospinal fluid (Li et al., 2004, Clinton et al., 2013). The mouse brain is the only organ where all forms of KL are detected: transmembrane, shed, and secreted (Imura et al., 2004, Clinton et al., 2013, Masso et al., 2015). Peripheral systems that characterized KL's functions showed that KL protein function varies with its form. Transmembrane KL is a co-receptor that transduces signaling of fibroblast growth factor 23 (FGF23) (Kurosu et al., 2006). Transmembrane KL is shed from cell surfaces into serum and cerebrospinal fluid (Imura et al., 2004, Chen et al., 2007, Yokoyama et al., 2015). Shed KL is acts as a sialidase (Cha et al., 2008, Cha et al., 2009) and a signaling pathway inhibitor (Kurosu et al., 2005, Liu et al., 2007, Doi et al., 2011, Zhou et al., 2013). The function of secreted KL remains unknown (Masso et al., 2015).

Little is known about the brain-specific mechanisms of KL action. We sought to determine whether KL is detected at the synapse, and found that transmembrane KL is a synaptic protein which could function to directly affect synaptic transmission. Thus we measured synaptic transmission before and after the onset KO and OE cognitive changes (Nagai et al., 2003, Dubal et al., 2014). We observed KL-mediated effects on both pre- and post-synaptic function of hippocampal CA1 Schaffer collateral neurons and attempted to rescue synaptic plasticity with acute application of shed KL.

Experimental Procedures

Animals

KL-deficient (KO,129S1/SvImJ) and overexpressing (OE,C57BL/6J) lines of mice are from M. Kuro-o (University of Texas Southwestern and Jichi Medical University, Japan). Strain-

specific, wild-type (WT) controls were used for all experiments. All mice were housed with free access to food and water at 26.6°C, humidity maintained above 40%. KO mice were supplemented with Bacon Softies or Nutra-gel (BioServ, Frenchtown, NJ) beginning week 5. All procedures were approved by the University of Alabama at Birmingham Institutional Animal Care and Use Committee.

Immunohistochemistry (IHC)

Mice were anesthetized and sacrificed by terminal perfusion followed by Bouin's fixation. IHC using paraffinized sections was performed as previously described (Clinton et al., 2013). IHC detection from perfused tissue underrepresents total KL protein within the brain as extracellular shed and secreted forms of the protein are likely cleared during tissue processing. Primary antibodies were incubated concurrently to detect KL (AF1819, R and D Systems, Minneapolis, MN) and microtubule associated protein 2 (Map2, SC20172, Santa Cruz Biotechnology, Dallas, TX) or phospho-neurofilament (SMI312, 837901, Biolegend, San Diego, CA). KL was detected after signal amplification with TSA-Cy3 (Perkin Elmer, Waltham, MA). Map2 and SMI312 were detected using species specific Alexa488 and mounted in Prolong Anti-fade mounting media (Thermo Fisher, Waltham, MA). Results were confirmed in 3 brains by imaging with an Olympus BX53 fluorescent (Center Valley, PA) or a confocal Zeiss laser scanning LSM510 microscope (Zeiss, Oberkochen, Germany).

Synaptosomes and synaptic membrane preparation

Mice were sacrificed by decapitation after inhalation anesthesia. Synaptosomes were isolated using discontinuous Percoll (GE Healthcare, Chicago, IL) gradients as described (Dunkley et al., 2008). Hippocampi were homogenized using a Teflon-coated pestle in sucrose buffer (0.32M sucrose, 1mM EDTA, 5mM Tris pH 7.4, 0.25mM DTT) with HALT protease inhibitor cocktail (PI78440, Thermo Fisher) and centrifuged at 1500×g. All centrifugation occurred at, 4°C. After reserving a supernatant aliquot for the input control, supernatant was layered on top of a discontinuous Percoll gradient (3%–23%, Percoll; 0.32M sucrose, 1mM EDTA, 5mM Tris pH 7.4, 0.25mM DTT). Membrane and synaptosomal fractions were generated by centrifugation at 46,000×g. Membrane samples derived from fractions above 10%. Synaptosomal samples derived from fractions pooled above 23%, Percoll diluted with sucrose buffer, and samples centrifuged at 29,000×g. Sucrose was removed by centrifugation and pellets were resuspended in RIPA buffer (150mM NaCl, 50mM Tris, pH 7.5, 1% Triton-X100, 0.5% sodium deoxycholate, 1% sodium dodecyl sulfate).

Synaptic membranes were prepared as described (Goebel-Goody et al., 2009, Dubal et al., 2014). Hippocampi were homogenized with a Teflon-coated pestle in sucrose buffer (320mM sucrose, 10mM Tris, pH 7.5, 1mM Na_3VO_4, 5mM NaF, 1mM EDTA and 1mM EGTA). The homogenate was centrifuged at 1,000×g and crude synaptosomal membrane pelleted by centrifugation at 10,000×g. The pellet was homogenized using a motorized pellet grinding pestle in sucrose buffer with 20 pulses and as extracted with 8 volumes of pellet buffer (0.5% Triton X100, 10mM Tris pH 7.5, 1mM Na_3VO4, 5mM NaF, 1mM EDTA and 1mM EGTA) before centrifugation at 32,000×g. Following centrifugation the post-synaptic density localized to the pellet and the presynaptic fraction to the supernatant. The pellet was

resuspended by sonication in sucrose buffer (with 1% SDS and 1X Halt protease inhibitor cocktail). The supernatant proteins were acetone concentrated overnight, separated from acetone, and resuspended by sonication into sucrose buffer containing 1% SDS and protease inhibitors.

Western blot

Synaptic fractions were prepared as above. Hippocampal lysates were prepared by homogenizing flash frozen tissue in RIPA buffer containing protease inhibitors. Following BCA assay (Thermo Fisher), 40–60μg of lysate or fraction was separated through 8% or 4–20% gradient polyacrylamide gels and transferred to nitrocellulose membranes (Thermo Fisher). Membranes were blocked with 5% non-fat dry milk in Tris buffered saline with 0.1% Tween 20 (TBST). Membranes were incubated in primary antibody (in 0.3% BSA in TBST) at 4°C overnight using antibodies to detect KL (KL2-34 (Maltare et al., 2014)), β-tubulin (Developmental Studies Hybridoma Bank, E7, Iowa City, IA), synaptophysin (Abcam, AB52636, Cambridge, MA), GluN1 (Neuromab, 75–272, Davis, CA) and SNAP25 (SC73044, Santa Cruz). Secondary antibodies conjugated to HRP were detected by chemiluminescence (Immobilon, Millipore, Billerica, MA) and exposure to film.

Recombinant shed KL function

HEK 293T cells (ATCC, Manassas, VA) were transfected with 200ng of TOP or FOP flash luciferase reporter plasmid (Veeman et al., 2003) (Addgene, Cambridge, MA: plasmids 12456 and 12457). Media containing 150ng/ml wnt3a with or without 400ng/ml of KL (R and D Systems, Minneapolis, MN) was incubated together overnight. Conditioned media was then replaced with media containing recombinant proteins. Cells were lysed and luminescence detected with the luciferase assay system (Promega, Madison, WI) and a Spectramax M3 (Molecular Devices, Sunnyvale, CA) 24 hours later. Results are reported as TOPflash/FOPflash of identical conditions from two independent experiments, 3 replicates/experiment.

Electrophysiology

Slice preparation—Mice were anesthetized and sacrificed at two time points for each strain based on the reported onset of cognitive impairment or enhancement (Nagai et al., 2003, Dubal et al., 2015). WT/KO mice were evaluated during the 5^{th} or 7^{th} week of life (Nagai et al., 2003). WT/OE mice were evaluated at 2 or 6 months of age (Dubal et al., 2014). Coronal vibratome sections (400 μm; VT1000S vibratome; Leica, Bannockburn, IL) were cut using ice-cold (1–3°C) dissecting solution (120mM NaCl, 3.5mM KCl, 0.7mM $CaCl_2$, 4.0mM $MgCl_2$, 1.25mM NaH_2PO4, 26mM $NaHCO_3$, and 10mM glucose; bubbled with 95% O_2/5% CO_2, pH 7.35–7.45). The CA3 region of the hippocampus was removed to prevent recurrent excitation. Using a holding chamber, slices were held at room temperature in dissecting solution and bubbled with 95% O_2/5% CO_2 for >1 h before recording. During the recordings, slices were held in a submersion recording chamber perfused with artificial cerebrospinal fluid (ACSF) (120mM NaCl, 3.5mM KCl, 2.5mM $CaCl_2$, 1.3mM $MgCl_2$, 1.25mM NaH_2PO4, 26mM NaHCO3 and 10mM glucose). All experiments were performed at ~ 30°C and experimenters were blind to genotype.

Field Potential Recording—Field excitatory postsynaptic potentials (fEPSPs) were recorded from *stratum radiatum* of CA1 using glass micropipettes (2–5 MΩ) filled with ACSF in response to extracellular stimulation of Schaffer Collateral axons by a bipolar tungsten microelectrode (FHC, Bowdoinham, ME, USA). Stimulation was generated by a Master-8-cp stimulator (A.P.I, Jerusalem, Israel) and applied with a BSI-2 biphasic stimulus isolator (BAK Electronics, Mount Airy, MD, USA). The initial slope of the fEPSP was used as a measure of synaptic response.

For measurement of paired-pulse facilitation, stimulation was applied as pairs of pulses (interval 40; 60; 100; 200; 500 ms or 50,100,150, 200, 250, 300ms) at 0.1 Hz. The paired-pulse ratio was calculated as fEPSP slope2/fEPSP slope1. ACSF contained picrotoxin (100 μm; Tocris, Bristol, UK) to block inhibitory $GABA_A$ receptors synaptic responses and 100 μm APV ([+]-2-amino-5-phosphonopentanoic acid; Tocris) to block NMDA receptor-mediated currents and prevent postsynaptic short-term plasticity, LTP, and long-term depression. Experiments using recombinant shed mouse KL (R and D systems, Minneapolis, MN) were recovered and recorded slices ACSF containing 5,000 pg/ml recombinant shed KL or diluent. A concentration ~5× physiological levels (Yamazaki et al., 2010) was selected to ensure that the sufficient protein reached the synapses during recovery/recording. Additional WT and KO slices were sequentially incubated for 10 minutes in 0, 500, 1,000, and 2,500 pg/ml of recombinant shed KL prior to PPF measurement.

Whole Cell Patch Clamp—Pyramidal cells in CA1 *stratum pyramidale* were identified visually using infrared differential inference contrast (IR-DIC) optics on a Nikon E600FN upright microscope (Nikon Inc.). In voltage clamp configuration, targeted neurons were patched and recorded at holding potential (−60 mV) using an Axopatch 200B amplifier (Axon Instruments, Sunnyvale, CA). Patch electrodes (4–6 MΩ) were filled with internal solution composed of: 100mM cesium gluconate, 0.6mM EGTA, 5.0mM $MgCl_2$, 10mM HEPES, 10mM BAPTA, 10mM ATP, 5mM QX-314; pH was adjusted to 7.2 with CsOH. Recordings were rejected if either access resistance or holding current increased more than 20% during the experiment.

Release probability—Release probability was assayed using the rate of block of NMDA EPSCs by the open channel blocker MK-801 ((5S,10R)-(+)-5-methyl-10,11-dihydro-5H-dibenzo[a,d]cyclohepten-5,10-imine maleate). NMDA receptor EPSCs were isolated by the addition of 10 μM NBQX to block AMPA/kainate receptors, and recorded at a holding potential of −40 mV after 0.1 Hz stimulation. The concentrations of ACSF calcium (2.5 mM) and magnesium (1.3 mM), were not changed and 100 μM picrotoxin was added to block fast inhibitory transmission. After a stable baseline was obtained, the membrane potential was held at −60 mV, 40 μM MK-801 added, and stimulation turned off for 10 min to allow MK-801equilibration. After that, the membrane potential was returned to −40 mV, stimulation was resumed at 0.1 Hz, and EPSCs were recorded for at least 160 stimuli. Stimulation at 0.1 Hz was used to avoid inducing short-term plasticity. A single exponential decay was fit to the EPSC amplitude versus stimulus number in MK-801 to obtain the decay constant (tau) for the MK-801 block. As MK-801 only blocks open NMDA receptors, the

rate of block is an indirect measure of the average release probability of the synapses (Hessler et al. 1993; Sun et al 2005; Speed and Dobrunz 2009).

NMDA/AMPA Current Ratio—In response to Shaffer collateral stimulation, NMDA/AMPA current ratios were measured in two steps for each CA1 pyramidal neuron. First, AMPA currents were measured at a holding potential of −70 mV in picrotoxin (100 μM); next, the holding potential was changed to +40 mV and NBQX was added to isolate NMDA currents. This was confirmed by reversible blockade by AP5 (100 μM). For each experiment, more than 10 traces of AMPA and NMDA responses were averaged, and the peak amplitudes measured.

LTP Experiments—5 and 7 week KO and 2 month OE LTP experiments were performed using an interface chamber (Fine Science Tools, Foster City, CA). Oxygenated ACSF (95%/5% O_2/CO_2; 120mM NaCl, 2.5mM KCl, 2mM $CaCl_2$, 1mM $MgCl_2$, 1.25mM NaH_2PO4, 25mM NaHCO3 and 25mM glucose) warmed to 30° C (TC-324B temperature controller, Warner Instruments, Hamden, CT) was perfused into the chamber at 1 ml/min. Electrophysiological traces were amplified (Model 1800 amplifier, A-M Systems, Sequim, WA), digitized and stored (Digidata models 1322A with Clampex software, Molecular Devices, Sunnyvale, CA). Extracellular stimuli were administered (Model 2200 stimulus isolator, A-M Systems) on the border of area CA3 and CA1 along the Schaffer-collaterals using enameled, bipolar platinum-tungsten (92%:8%) electrodes. fEPSPs were recorded in *stratum radiatum* with an ACSF-filled glass recording electrode (1–3 MΩ). The relationship between fiber volley and fEPSP slopes over various stimulus intensities (0.5 V – 15 V, 25 nA – 1.5 μA) was used to assess baseline synaptic transmission. High-frequency stimulus-induced LTP was induced by administering 3, 100 Hz tetani (1 sec duration) at an interval of 20 sec. Synaptic efficacy was monitored 20 min prior to and 1–3 h following induction of LTP by recording fEPSPs every 20 sec (traces were averaged for every 2 min interval).

6 month OE LTP experiments were performed using a submersion chamber (Warner Instruments, Hamden, CT) with oxygenated ACSF (120mM NaCl, 3.5mM KCl, 2.5mM $CaCl_2$, 1.3mM $MgCl_2$, 1.25mM NaH_2PO4, 26mM NaHCO3 and 10mM glucose) warmed to ~30°C (TC-344B temperature controller, Warner Instruments, Hamden, CT) flowing at 1 ml/min. fEPSPs were recorded from *stratum radiatum* of CA1 using glass micropipettes (2–5 MΩ) filled with ACSF in response to extracellular stimulation of Schaffer Collateral axons by a bipolar tungsten microelectrode (FHC, Bowdoinham, ME, USA). Stimulation was generated by a Master-8-cp stimulator (A.P.I, Jerusalem, Israel) and applied with a BSI-2 biphasic stimulus isolator (BAK Electronics, Mount Airy, MD, USA). Baseline fEPSP was recorded at 20 sec interval for 20 min and the stimulation intensity was set to obtain a response at 50% of the maximum synaptic response (before the onset of polysynaptic EPSCs). LTP was induced by 3 repeats of 100 Hz tetanic stimulation (100 pulses) with a 20 sec interval. Recording after tetanic stimulation lasted for an hour at 20 sec interval and data binned every 2 min.

Statistical Analysis

Data are presented as mean ± standard error of the mean. Statistical comparisons were made using the Student's *t*-test, with $p < 0.05$ considered significant.

Results

Synaptic membranes contain Klotho

First, we confirmed that KL is generated by multiple cell types within the brain of WT but not KO mice (Figure 1). Consistent with previous reports (Li et al., 2004, Maltare et al., 2014), choroid plexus KL immunoreactivity is most intense (Figure 1A). Although less highly expressed than choroid plexus, throughout subfields of the hippocampus, neuronal cell bodies and processes express KL (Figure 1B). CA1 neurons prominently show that KL co-localizes with dendritic marker Map2 but not axonal marker SMI312 (Figures 1B–E). Thus, by IHC, neuronal KL localizes to dendrites but not axons of CA1 hippocampal neurons.

Western blot of 7 week old wild-type (WT) but not KO total hippocampal lysates detected full length KL protein (Figure 2A). As expected, OE hippocampal KL expression was increased relative to strain-specific WT control (Figure 2A). To determine whether transmembrane KL localizes to hippocampal membranes, we fractionated individual hippocampi. Percoll gradients were used to separate cell membrane from synaptosomal fractions (Dunkley et al., 2008). Membrane and synaptosome fractions show transmembrane KL by Western blot of WT but not KO hippocampi (Figure 2B). Our IHC suggests KL localizes to the post-synapse. However, when we separated synaptic membranes into pre- and post-synaptic fractions (Goebel-Goody et al., 2009, Dubal et al., 2014), WT but not KO fractions both showed KL (Figure 2C). Similar results were obtained when fractionating WT and OE hippocampi by Percoll or isolating synaptic membranes (Figure 2D,E). Together these experiments show that both pre and post-synaptic hippocampal neuron membranes contain KL.

The absence of KL causes age-dependent enhancement of short and long-term plasticity

To determine if KL effects synaptic transmission, we measured WT and KO synaptic function before and after the onset of cognitive impairment. We first tested CA1 hippocampal synaptic plasticity using acute slices from 5 week old WT and KO mice to measure function before the onset of cognitive impairment. To test for general synaptic function deficits, we examined the input-output (I/O) relationship of Schaffer collateral synapses using field potential recordings in response to single electrical stimuli. Measuring initial slopes of the evoked fEPSP as function of the fiber volley amplitude, the I/O relationship between WT and KO was not different, indicating no basal synaptic transmission change (Figure 3A).

We next tested 5 week olds for effects on paired-pulse facilitation (PPF), a simple form of presynaptic short-term plasticity, and found increased PPF at KO synapses compared to WT (Figure 3B). As PPF is usually inversely related to initial release probability (Dobrunz and Stevens, 1997, Zucker and Regehr, 2002), enhanced PPF suggests that the initial release

probability might be lower at KO synapses. Thus we performed whole-cell patch clamp recordings of CA1 pyramidal neurons in the presence of the use-dependent antagonist NMDA receptor MK-801 to measure the rate of NMDA receptor block (Hessler et al., 1993, Sun and Dobrunz, 2006, Speed and Dobrunz, 2009). The rate of blocking is an indirect measure of average synaptic release probability (Hessler et al., 1993) with decreased release probability causing a slower blocking rate of MK-801 NMDA EPSCs. However, there is no initial release probability change as no significant difference was observed between the WT and KO MK-801 blocking curves (Figure 3D,E).

To test long-term plasticity, we compared LTP at Schaffer collateral synapses from 5 week old WT and KO mice. LTP was measured after high frequency stimulation (three 100 Hz tetani of 1 sec duration, separated by 20 sec) using field potential recordings. KO slices showed enhanced post-tetanic potentiation and LTP compared to WT (Figure 3C). The increased KO LTP magnitude persisted for more than an hour (Figure 3C). Because increased NMDA/AMPA ratio can cause enhanced LTP (Smith and McMahon, 2005, 2006), we tested CA1 pyramidal cells for differences in the evoked NMDA/AMPA current ratio. There was no significant NMDA/AMPA ratio difference (Figure 3F), indicating that the NMDA/AMPA ratio change does not underlie the enhanced KO LTP.

To determine if synaptic transmission is also altered after the onset of cognitive impairment, we tested synaptic transmission of older cognitively impaired KO mice (7 weeks). The I/O curve did not change (data not shown) and the 5 week increased PPF and LTP were no longer detected at 7 weeks (Figure 3G, H). Together, these data show that enhanced KO short-term and long-term synaptic plasticity rapidly declines over shortened mouse lifespan and that KL is important for normal synaptic plasticity.

KL overexpression causes age-dependent increased LTP

By 4–6 months old, OE mice have both increased hippocampal-dependent memory and enhanced dentate gyrus LTP (Dubal et al., 2014). However, it is not known if OE CA1 long-term plasticity is similarly affected, if changes in synaptic plasticity correlate with the onset of cognitive enhancement, or whether short-term plasticity is regulated by KL overexpression. We tested WT and OE slices for short-term and long-term synaptic plasticity at Schaffer collateral synapses at 2 and 6 month olds. Neither I/O curves (data not shown) nor PPF were different between WT and OE mice at either age (Figure 4A,C). At 2 months of age, LTP was also not different between WT and OE mice (Figure 4B). However, by 6 months of age, CA1 synapses show impaired LTP (Figure 4D). These data indicate that with age, reduced long-term synaptic plasticity occurs upon KL overexpression.

Acute application of shed KL does not affect short term plasticity

As the synaptic compartment contains transmembrane KL, we would assume that it functions to mediate synaptic plasticity. However, it is possible that shed KL mediates these effects or could act acutely to further modify synaptic efficacy. Recombinant shed KL was tested for function by transfecting HEK 293T cells with TOPflash or FOPflash reporter plasmid and incubating cells with recombinant Wnt3a alone or with recombinant shed KL. Wnt signal transduction was reduced by the presence of shed KL confirming that

recombinant protein is functional (Figure 5A) (Liu et al., 2007). To determine whether shed KL could affect PPF acutely, we added shed recombinant KL to ACSF during recovery and recording. Acute shed KL had no effect on the enhanced KO PPF (Figure 5B). Likewise, shed KL had no acute effect on WT PPF (Figure 5C). To ensure that the lack of a response was not a consequence of higher than physiological levels of KL, additional slices were incubated in increasing concentrations of recombinant shed KL (0–2,500 pg/ml). PPF was measured at each concentration and did not change compared to baseline for either KO (Figure 5D) or WT (data not shown) slices. These data suggest that there are no acute effects of shed KL on short-term synaptic plasticity.

Discussion

Our data show that hippocampal neurons express KL and synaptic membranes contain the full length protein (Figure 1,2). KL-deficiency enhances pre- and post-synaptic plasticity of Schaffer collateral neurons prior to the onset of cognitive impairment but without affecting initial release probability or NMDA/AMPA ratios (Figure 3). Enhanced plasticity rapidly degrades over the two weeks during which cognitive impairment develops and animals undergo terminal decline to death (Figure 3). Acute effects of shed KL neither restore baseline KO PPF nor affected WT PPF (Figure 5). When KL is overexpressed neither an effect on young animal LTP nor an effect on short-term plasticity at either age was measured (Figure 4). However, overexpression induced the inverse effect on long-term plasticity, decreasing 6 month old OE LTP (Figure 4). Together these data show that increasing and decreasing KL alters synaptic function and implicate a direct role for KL protein in synaptic plasticity. KL is downregulated with aging (Duce et al., 2008, Yamazaki et al., 2010), and our data suggest that age-related loss of KL would impact synaptic functions important for learning and memory.

Our results show that KL-deficiency affects both short-term plasticity (typically mediated by pre-synaptic mechanisms) and long-term plasticity (typically mediated by post-synaptic mechanisms). Although PPF enhancement is often caused by altering initial release probability (Zucker and Regehr, 2002, Sun et al., 2005, Speed and Dobrunz, 2009), data from our MK-801 experiment showed no difference (Figure 3D,E). PPF change without a concurrent initial release probability change is reported and when reported, the underlying mechanism remains pre-synaptic (e.g. (Kokaia et al., 1998, Sippy et al., 2003, Sun and Dobrunz, 2006, Speed and Dobrunz, 2009, Schiess et al., 2010, Walters et al., 2014). Our data are consistent with the previous study that measured 7 week KO LTP and found no change with a similar stimulation pattern, rather only when neurons were lightly stimulated by a single theta burst (Park et al., 2013). As KL is suggested to modify GluN2B expression (Dubal et al., 2014), we tested whether the KO mice had an enhanced NMDA/AMPA ratio that could underlie enhanced LTP, but found no change (Figure 3F). Although further studies will be needed to determine the mechanism by which KL-deficiency enhances long-term plasticity, nearly all mechanisms of LTP change are post-synaptic.

In the OE, only post-synaptic functional effects were measured, consistent with the previous report from dentate gyrus synapses (Dubal et al., 2014). It is likely that pre-synaptic KL function is maximal at normal KL levels but that overexpression can impact post-synaptic

LTP. The effect of overexpression on LTP is opposite of dentate gyrus change (Dubal et al., 2014), indicating that the effects of KL on synaptic plasticity are region-specific. It is unclear why effects of overexpression are not observed until 4–6 months of age but our data suggest that KL overexpression does not affect brain function until adulthood.

Although cognitive function is clearly inversely affected by KL expression level (Nagai et al., 2003, Dubal et al., 2014), it is unclear which form of KL mediates effects. Current global KL-deficient and overexpressing mouse models manipulate all forms of KL, making it difficult to assign specific function to KL protein forms. Our data show KL protein at the size of the full length, transmembrane protein fractionates with both pre and post-synaptic membrane proteins (Figure 2). These and our KO electrophysiology results demonstrate that KL has functional effects on both sides of the synapse suggesting a hippocampal synaptic plasticity role for transmembrane KL. Additionally, bath application of shed KL did not rescue the enhanced KO PPF nor alter WT PPF, suggesting that the shed form does not have acute effects, although these data do not rule out possible long-term synaptic effects of more or less shed KL. It is unclear what drives the rapid and dramatic loss of synaptic enhancement within the KO brain between weeks 5 to 7. We know that increased oxidative stress develops during this time, the amelioration of which blocks development of cognitive impairment (Nagai et al., 2003). In addition, KL-deficiency causes decreased hippocampal cholinergic signaling, which also could contribute (Park et al., 2013).

As KO mice show rapid onset cognitive impairment (Nagai et al., 2003) and OE mice develop improved hippocampal-dependent cognitive function (Dubal et al., 2014), our synaptic plasticity results were surprising as we did not observe the common correlation of decreased plasticity with decreased cognitive performance and vice versa (Lu et al., 1997, Saxe et al., 2006, Lee and Silva, 2009, Wang et al., 2009, Han et al., 2013). Although less common, many examples exist of genetic manipulations that result in increased synaptic plasticity, particularly increased LTP, with decreased spatial memory (Kaksonen et al., 2002, Pineda et al., 2004, Niisato et al., 2005, Rutten et al., 2008, Kim et al., 2009). But none of those studies saw a concurrent PPF effect. Increases in both PPF and LTP, with enhanced spatial memory are reported in the Chordin knockout (Sun et al., 2007) and MECP2 overexpressing (Collins et al., 2004) mice.

In rat slice culture, increased PPF and LTP were measured upon bath application of FGF1 protein (Sasaki et al., 1994). This occurs through activation of PKC, suggesting that the increased short and long-term plasticity are caused by signaling changes downstream of post-synaptic receptor activation. Similarly, increased PPF and LTP with impaired spatial memory, occurred upon genetic manipulation of PSD-95 in a mouse model engineered to express only the first two PDZ protein interaction domains of PSD-95 (Migaud et al., 1998). Although no mechanism of action was defined, again, signaling downstream of NMDA receptor activation was implicated (Migaud et al., 1998). Cell adhesion molecules like pre-synaptic neurexin, bind to post-synaptic neuroligin. Synaptic neuroligin proteins interact with PSD-95 and thus could mediate retrograde feedback from the post-synaptic density (Migaud et al., 1998). As transmembrane KL is a predominately extracellular protein, it could be a synaptic cell adhesion protein and thus promote retrograde signaling from the post-synapse. Furthermore, as KL overexpression correlates with increased NR2B receptors

(Dubal et al., 2014), KL expression could mediate NMDA signaling from the post-synaptic density. The unusual KO synaptic phenotype of enhanced PPF and LTP with early onset cognitive impairment indicate that KL is important for synaptic plasticity. As it is a naturally age-downregulated protein (Duce et al., 2008, Yamazaki et al., 2010), further defining its mechanism of action at the synapse is important to understanding age-related hippocampal dysfunction.

Acknowledgments

Work was supported by the National Institutes of Health grants R56AG052936 and R00AG034989 to GDK and a Civitan International Emerging Scholar Grant to HV.

Abbreviations

AMPA	α-amino-3-hydroxy-5methyl-4-isoxazolepropionic acid receptor
fEPSP	field excitatory post-synaptic potential
EPSC	excitatory post-synaptic current
Hz	hertz
I/O	input/output
KL	klotho
KO	Klotho-deficient mouse
LTP	long-term potentiation
MAP2	microtubule associated protein 2
min	minute
MK-801	((5S,10R)-(+)-5-methyl-10,11-dihydro-5H-dibenzo[a,d]cyclohepten-5,10-imine maleate
ml	milliliter
ms	millisecond
mV	millivolt
NMDA	N-methyl D-aspartate receptor beta 2 subunit
OE	KL overexpressor mouse
sec	second
PPF	paired-pulse facilitation
SMI312	neurofilament antibody
WT	wild-type mouse

References

Arking DE, Krebsova A, Macek M Sr, Macek M Jr, Arking A, Mian IS, Fried L, Hamosh A, Dey S, McIntosh I, Dietz HC. Association of human aging with a functional variant of klotho. Proc Natl Acad Sci U S A. 2002; 99:856–861. [PubMed: 11792841]

Brobey RK, German D, Sonsalla PK, Gurnani P, Pastor J, Hsieh CC, Papaconstantinou J, Foster PP, Kuro-o M, Rosenblatt KP. Klotho Protects Dopaminergic Neuron Oxidant-Induced Degeneration by Modulating ASK1 and p38 MAPK Signaling Pathways. PLoS One. 2015; 10:e0139914. [PubMed: 26452228]

Cha SK, Hu MC, Kurosu H, Kuro-o M, Moe O, Huang CL. Regulation of renal outer medullary potassium channel and renal K(+) excretion by Klotho. Mol Pharmacol. 2009; 76:38–46. [PubMed: 19349416]

Cha SK, Ortega B, Kurosu H, Rosenblatt KP, Kuro OM, Huang CL. Removal of sialic acid involving Klotho causes cell-surface retention of TRPV5 channel via binding to galectin-1. Proc Natl Acad Sci U S A. 2008; 105:9805–9810. [PubMed: 18606998]

Chen CD, Podvin S, Gillespie E, Leeman SE, Abraham CR. Insulin stimulates the cleavage and release of the extracellular domain of Klotho by ADAM10 and ADAM17. Proc Natl Acad Sci U S A. 2007; 104:19796–19801. [PubMed: 18056631]

Chen CD, Sloane JA, Li H, Aytan N, Giannaris EL, Zeldich E, Hinman JD, Dedeoglu A, Rosene DL, Bansal R, Luebke JI, Kuro-o M, Abraham CR. The antiaging protein Klotho enhances oligodendrocyte maturation and myelination of the CNS. J Neurosci. 2013; 33:1927–1939. [PubMed: 23365232]

Clinton SM, Glover ME, Maltare A, Laszczyk AM, Mehi SJ, Simmons RK, King GD. Expression of klotho mRNA and protein in rat brain parenchyma from early postnatal development into adulthood. Brain Res. 2013; 1527:1–14. [PubMed: 23838326]

Collins AL, Levenson JM, Vilaythong AP, Richman R, Armstrong DL, Noebels JL, David Sweatt J, Zoghbi HY. Mild overexpression of MeCP2 causes a progressive neurological disorder in mice. Hum Mol Genet. 2004; 13:2679–2689. [PubMed: 15351775]

Dobrunz LE, Stevens CF. Heterogeneity of release probability, facilitation, and depletion at central synapses. Neuron. 1997; 18:995–1008. [PubMed: 9208866]

Doi S, Zou Y, Togao O, Pastor JV, John GB, Wang L, Shiizaki K, Gotschall R, Schiavi S, Yorioka N, Takahashi M, Boothman DA, Kuro-o M. Klotho inhibits transforming growth factor-beta1 (TGF-beta1) signaling and suppresses renal fibrosis and cancer metastasis in mice. J Biol Chem. 2011; 286:8655–8665. [PubMed: 21209102]

Dubal DB, Yokoyama JS, Zhu L, Broestl L, Worden K, Wang D, Sturm VE, Kim D, Klein E, Yu GQ, Ho K, Eilertson KE, Yu L, Kuro-o M, De Jager PL, Coppola G, Small GW, Bennett DA, Kramer JH, Abraham CR, Miller BL, Mucke L. Life extension factor klotho enhances cognition. Cell Rep. 2014; 7:1065–1076. [PubMed: 24813892]

Dubal DB, Zhu L, Sanchez PE, Worden K, Broestl L, Johnson E, Ho K, Yu GQ, Kim D, Betourne A, Kuro OM, Masliah E, Abraham CR, Mucke L. Life Extension Factor Klotho Prevents Mortality and Enhances Cognition in hAPP Transgenic Mice. J Neurosci. 2015; 35:2358–2371. [PubMed: 25673831]

Duce JA, Podvin S, Hollander W, Kipling D, Rosene DL, Abraham CR. Gene profile analysis implicates Klotho as an important contributor to aging changes in brain white matter of the rhesus monkey. Glia. 2008; 56:106–117. [PubMed: 17963266]

Dunkley PR, Jarvie PE, Robinson PJ. A rapid Percoll gradient procedure for preparation of synaptosomes. Nat Protoc. 2008; 3:1718–1728. [PubMed: 18927557]

Goebel-Goody SM, Davies KD, Alvestad Linger RM, Freund RK, Browning MD. Phospho-regulation of synaptic and extrasynaptic N-methyl-d-aspartate receptors in adult hippocampal slices. Neuroscience. 2009; 158:1446–1459. [PubMed: 19041929]

Han X, Chen M, Wang F, Windrem M, Wang S, Shanz S, Xu Q, Oberheim NA, Bekar L, Betstadt S, Silva AJ, Takano T, Goldman SA, Nedergaard M. Forebrain engraftment by human glial progenitor cells enhances synaptic plasticity and learning in adult mice. Cell Stem Cell. 2013; 12:342–353. [PubMed: 23472873]

Hessler NA, Shirke AM, Malinow R. The probability of transmitter release at a mammalian central synapse. Nature. 1993; 366:569–572. [PubMed: 7902955]

Imura A, Iwano A, Tohyama O, Tsuji Y, Nozaki K, Hashimoto N, Fujimori T, Nabeshima Y. Secreted Klotho protein in sera and CSF: implication for post-translational cleavage in release of Klotho protein from cell membrane. FEBS Lett. 2004; 565:143–147. [PubMed: 15135068]

Kaksonen M, Pavlov I, Voikar V, Lauri SE, Hienola A, Riekki R, Lakso M, Taira T, Rauvala H. Syndecan-3-deficient mice exhibit enhanced LTP and impaired hippocampus-dependent memory. Mol Cell Neurosci. 2002; 21:158–172. [PubMed: 12359158]

Kim MH, Choi J, Yang J, Chung W, Kim JH, Paik SK, Kim K, Han S, Won H, Bae YS, Cho SH, Seo J, Bae YC, Choi SY, Kim E. Enhanced NMDA receptor-mediated synaptic transmission, enhanced long-term potentiation, and impaired learning and memory in mice lacking IRSp53. J Neurosci. 2009; 29:1586–1595. [PubMed: 19193906]

Kokaia M, Asztely F, Olofsdotter K, Sindreu CB, Kullmann DM, Lindvall O. Endogenous neurotrophin-3 regulates short-term plasticity at lateral perforant path-granule cell synapses. J Neurosci. 1998; 18:8730–8739. [PubMed: 9786980]

Kuro-o M, Matsumura Y, Aizawa H, Kawaguchi H, Suga T, Utsugi T, Ohyama Y, Kurabayashi M, Kaname T, Kume E, Iwasaki H, Iida A, Shiraki-Iida T, Nishikawa S, Nagai R, Nabeshima YI. Mutation of the mouse klotho gene leads to a syndrome resembling ageing. Nature. 1997; 390:45–51. [PubMed: 9363890]

Kurosu H, Ogawa Y, Miyoshi M, Yamamoto M, Nandi A, Rosenblatt KP, Baum MG, Schiavi S, Hu MC, Moe OW, Kuro-o M. Regulation of fibroblast growth factor-23 signaling by klotho. J Biol Chem. 2006; 281:6120–6123. [PubMed: 16436388]

Kurosu H, Yamamoto M, Clark JD, Pastor JV, Nandi A, Gurnani P, McGuinness OP, Chikuda H, Yamaguchi M, Kawaguchi H, Shimomura I, Takayama Y, Herz J, Kahn CR, Rosenblatt KP, Kuro-o M. Suppression of aging in mice by the hormone Klotho. Science. 2005; 309:1829–1833. [PubMed: 16123266]

Lee YS, Silva AJ. The molecular and cellular biology of enhanced cognition. Nat Rev Neurosci. 2009; 10:126–140. [PubMed: 19153576]

Li SA, Watanabe M, Yamada H, Nagai A, Kinuta M, Takei K. Immunohistochemical localization of Klotho protein in brain, kidney, and reproductive organs of mice. Cell Struct Funct. 2004; 29:91–99. [PubMed: 15665504]

Liu H, Fergusson MM, Castilho RM, Liu J, Cao L, Chen J, Malide D, Rovira II, Schimel D, Kuo CJ, Gutkind JS, Hwang PM, Finkel T. Augmented Wnt signaling in a mammalian model of accelerated aging. Science. 2007; 317:803–806. [PubMed: 17690294]

Lu YM, Jia Z, Janus C, Henderson JT, Gerlai R, Wojtowicz JM, Roder JC. Mice lacking metabotropic glutamate receptor 5 show impaired learning and reduced CA1 long-term potentiation (LTP) but normal CA3 LTP. J Neurosci. 1997; 17:5196–5205. [PubMed: 9185557]

Maltare A, Nietz AK, Laszczyk AM, Dunn TS, Ballestas ME, Accavitti-Loper MA, King GD. Development and characterization of monoclonal antibodies to detect klotho. Monoclon Antib Immunodiagn Immunother. 2014; 33:420–427. [PubMed: 25513981]

Masso A, Sanchez A, Gimenez-Llort L, Lizcano JM, Canete M, Garcia B, Torres-Lista V, Puig M, Bosch A, Chillon M. Secreted and Transmembrane alphaKlotho Isoforms Have Different Spatio-Temporal Profiles in the Brain during Aging and Alzheimer's Disease Progression. PLoS One. 2015; 10:e0143623. [PubMed: 26599613]

Migaud M, Charlesworth P, Dempster M, Webster LC, Watabe AM, Makhinson M, He Y, Ramsay MF, Morris RG, Morrison JH, O'Dell TJ, Grant SG. Enhanced long-term potentiation and impaired learning in mice with mutant postsynaptic density-95 protein. Nature. 1998; 396:433–439. [PubMed: 9853749]

Nagai T, Yamada K, Kim HC, Kim YS, Noda Y, Imura A, Nabeshima Y, Nabeshima T. Cognition impairment in the genetic model of aging klotho gene mutant mice: a role of oxidative stress. Faseb J. 2003; 17:50–52. [PubMed: 12475907]

Niisato K, Fujikawa A, Komai S, Shintani T, Watanabe E, Sakaguchi G, Katsuura G, Manabe T, Noda M. Age-dependent enhancement of hippocampal long-term potentiation and impairment of spatial

learning through the Rho-associated kinase pathway in protein tyrosine phosphatase receptor type Z-deficient mice. J Neurosci. 2005; 25:1081–1088. [PubMed: 15689543]

Park SJ, Shin EJ, Min SS, An J, Li Z, Hee Chung Y, Hoon Jeong J, Bach JH, Nah SY, Kim WK, Jang CG, Kim YS, Nabeshima Y, Nabeshima T, Kim HC. Inactivation of JAK2/STAT3 signaling axis and downregulation of M1 mAChR cause cognitive impairment in klotho mutant mice, a genetic model of aging. Neuropsychopharmacology : official publication of the American College of Neuropsychopharmacology. 2013; 38:1426–1437. [PubMed: 23389690]

Pineda VV, Athos JI, Wang H, Celver J, Ippolito D, Boulay G, Birnbaumer L, Storm DR. Removal of G(ialpha1) constraints on adenylyl cyclase in the hippocampus enhances LTP and impairs memory formation. Neuron. 2004; 41:153–163. [PubMed: 14715142]

Rutten K, Misner DL, Works M, Blokland A, Novak TJ, Santarelli L, Wallace TL. Enhanced long-term potentiation and impaired learning in phosphodiesterase 4D-knockout (PDE4D) mice. Eur J Neurosci. 2008; 28:625–632. [PubMed: 18702734]

Sasaki K, Oomura Y, Figurov A, Yagi H. Acidic fibroblast growth factor facilitates generation of long-term potentiation in rat hippocampal slices. Brain Res Bull. 1994; 33:505–511. [PubMed: 7514484]

Saxe MD, Battaglia F, Wang JW, Malleret G, David DJ, Monckton JE, Garcia AD, Sofroniew MV, Kandel ER, Santarelli L, Hen R, Drew MR. Ablation of hippocampal neurogenesis impairs contextual fear conditioning and synaptic plasticity in the dentate gyrus. Proceedings of the National Academy of Sciences of the United States of America. 2006; 103:17501–17506. [PubMed: 17088541]

Schiess AR, Scullin C, Partridge LD. Maturation of Schaffer collateral synapses generates a phenotype of unreliable basal evoked release and very reliable facilitated release. Eur J Neurosci. 2010; 31:1377–1387. [PubMed: 20384768]

Shiozaki M, Yoshimura K, Shibata M, Koike M, Matsuura N, Uchiyama Y, Gotow T. Morphological and biochemical signs of age-related neurodegenerative changes in klotho mutant mice. Neuroscience. 2008; 152:924–941. [PubMed: 18343589]

Sippy T, Cruz-Martin A, Jeromin A, Schweizer FE. Acute changes in short-term plasticity at synapses with elevated levels of neuronal calcium sensor-1. Nat Neurosci. 2003; 6:1031–1038. [PubMed: 12947410]

Smith CC, McMahon LL. Estrogen-induced increase in the magnitude of long-term potentiation occurs only when the ratio of NMDA transmission to AMPA transmission is increased. J Neurosci. 2005; 25:7780–7791. [PubMed: 16120779]

Smith CC, McMahon LL. Estradiol-induced increase in the magnitude of long-term potentiation is prevented by blocking NR2B-containing receptors. J Neurosci. 2006; 26:8517–8522. [PubMed: 16914677]

Speed HE, Dobrunz LE. Developmental changes in short-term facilitation are opposite at temporoammonic synapses compared to Schaffer collateral synapses onto CA1 pyramidal cells. Hippocampus. 2009; 19:187–204. [PubMed: 18777561]

Sun HY, Dobrunz LE. Presynaptic kainate receptor activation is a novel mechanism for target cell-specific short-term facilitation at Schaffer collateral synapses. J Neurosci. 2006; 26:10796–10807. [PubMed: 17050718]

Sun HY, Lyons SA, Dobrunz LE. Mechanisms of target-cell specific short-term plasticity at Schaffer collateral synapses onto interneurones versus pyramidal cells in juvenile rats. J Physiol. 2005; 568:815–840. [PubMed: 16109728]

Sun M, Thomas MJ, Herder R, Bofenkamp ML, Selleck SB, O'Connor MB. Presynaptic contributions of chordin to hippocampal plasticity and spatial learning. J Neurosci. 2007; 27:7740–7750. [PubMed: 17634368]

Veeman MT, Slusarski DC, Kaykas A, Louie SH, Moon RT. Zebrafish prickle, a modulator of noncanonical Wnt/Fz signaling, regulates gastrulation movements. Curr Biol. 2003; 13:680–685. [PubMed: 12699626]

Walters BJ, Hallengren JJ, Theile CS, Ploegh HL, Wilson SM, Dobrunz LE. A catalytic independent function of the deubiquitinating enzyme USP14 regulates hippocampal synaptic short-term plasticity and vesicle number. J Physiol. 2014; 592:571–586. [PubMed: 24218545]

Wang D, Cui Z, Zeng Q, Kuang H, Wang LP, Tsien JZ, Cao X. Genetic enhancement of memory and long-term potentiation but not CA1 long-term depression in NR2B transgenic rats. PLoS One. 2009; 4:e7486. [PubMed: 19838302]

Yamazaki Y, Imura A, Urakawa I, Shimada T, Murakami J, Aono Y, Hasegawa H, Yamashita T, Nakatani K, Saito Y, Okamoto N, Kurumatani N, Namba N, Kitaoka T, Ozono K, Sakai T, Hataya H, Ichikawa S, Imel EA, Econs MJ, Nabeshima Y. Establishment of sandwich ELISA for soluble alpha-Klotho measurement: Age-dependent change of soluble alpha-Klotho levels in healthy subjects. Biochem Biophys Res Commun. 2010; 398:513–518. [PubMed: 20599764]

Yokoyama JS, Sturm VE, Bonham LW, Klein E, Arfankis K, Yu L, Coppola G, Kramer JH, Bennett DA, Miller BL, Dubal DB. Variation in longeivity gene KLOTHO is associated with greater cortical volumes. Annals of Clinical and Translational Neurology. 2015; 2:215–230. [PubMed: 25815349]

Zeldich E, Chen CD, Colvin TA, Bove-Fenderson EA, Liang J, Tucker Zhou TB, Harris DA, Abraham CR. The neuroprotective effect of Klotho is mediated via regulation of members of the redox system. The Journal of biological chemistry. 2014; 289:24700–24715. [PubMed: 25037225]

Zhou L, Li Y, Zhou D, Tan RJ, Liu Y. Loss of Klotho contributes to kidney injury by derepression of Wnt/beta-catenin signaling. J Am Soc Nephrol. 2013; 24:771–785. [PubMed: 23559584]

Zucker RS, Regehr WG. Short-term synaptic plasticity. Annu Rev Physiol. 2002; 64:355–405. [PubMed: 11826273]

Highlights

- Klotho is detected in synaptosomes isolated from hippocampus
- Enhanced CA1 paired-pulse facilitation and long-term potentiation precede cognitive impairment in Klotho-deficient mice.
- Klotho overexpression does not affect pre-synaptic plasticity but decreases long-term potentiation at CA1 synapses.

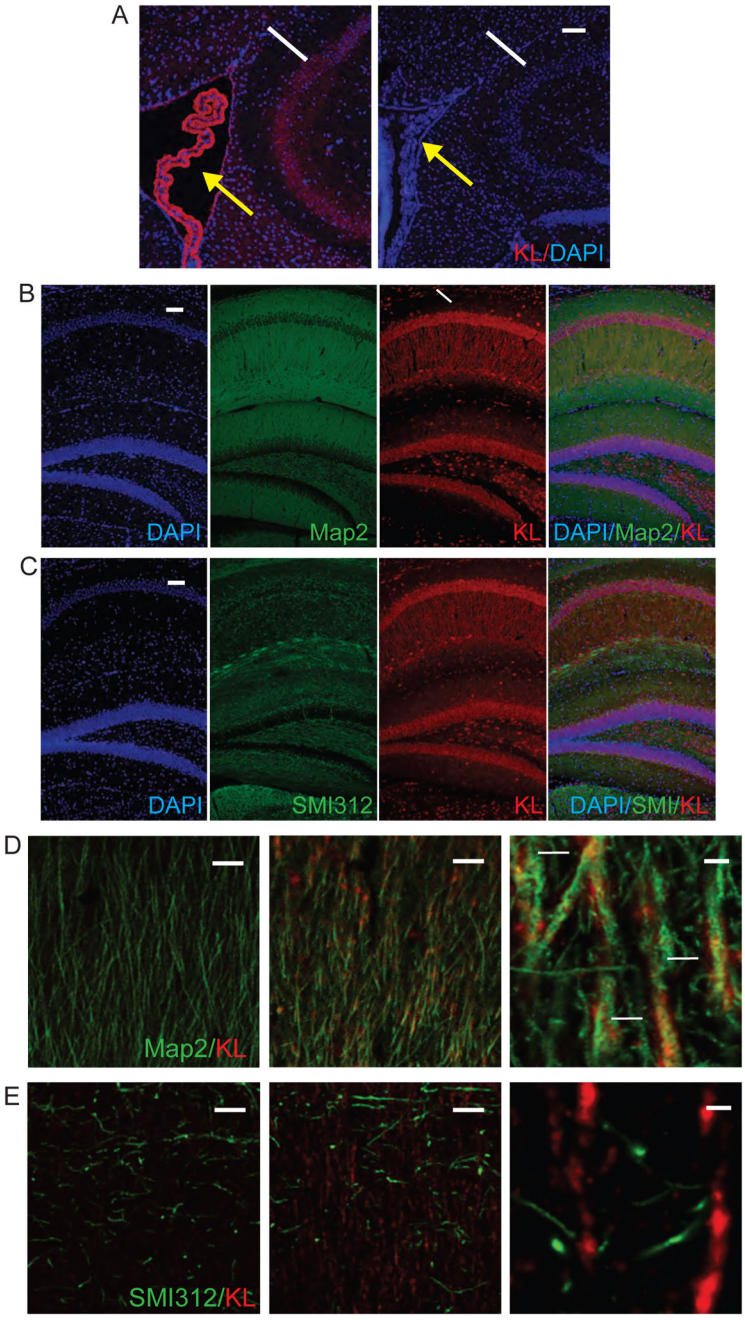

Figure 1. Hippocampal neurons express KL

A. Representative images of WT KL expression (red) in choroid plexus (yellow arrows) and adjacent hippocampal CA1 neurons (white arrow). KO brains show no KL expression. **B.** Hippocampal expression of KL (red) localizes to WT dendrites (Map2; dendrites), white arrow indicates the CA1 region. **C**. Hippocampal expression of KL (red) does not localizes to WT axons (SMI312; green). **D.** Dendritic co-localization within WT CA1 hippocampal dendrites (KL (red) and Map2 (green; dendrites)), with increasing magnification. Co-localization indicated with white arrows. **E**. Lack of axonal co-localization within WT CA1 axons KL (red) and SMI312 (green), with increasing magnification. Nuclei are

counterstained with DAPI (blue). D and E are representative single plane, confocal images. Scale bars represent 100μm in A, B, and C; D and E 50μm left and middle or 5μm right.

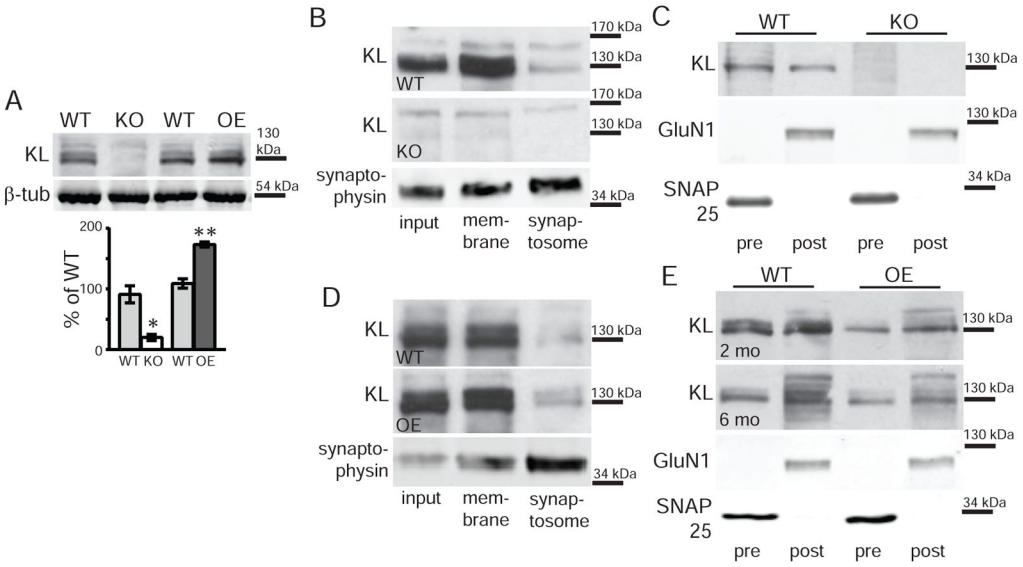

Figure 2. Synaptic fractions contain KL

A. KL (130kDa) detected by Western blot from whole hippocampal lysates of 2 month old WT and OE but not KO brains. WT are strain-specific throughout as detailed in methods. β-tubulin (51kDa) used as a loading control. Lines represent the nearest molecular weight marker. Quantification represents average band intensity normalized to GAPDH and expressed as % of the relevant WT control (n=3). **B**. Western blot detecting KL from synaptosome fractions of 2 month old WT but not KO hippocampi. Representative WT synaptophysin (38kDa) blot verifies synaptic protein enrichment. Input: pre-fractionation lysate, membrane: fraction containing membrane proteins, synaptosome: fraction enriched for synaptic proteins. **C**. Western blot detecting KL from WT but not KO hippocampal pre-synaptic (pre) and post-synaptic (post) fractions. Presynaptic enrichment validated using SNAP25 (25 kDa) and post-synaptic enrichment using GluN1 (110 kDa). **D**. Western blot detecting KL in synaptosome fractions from 2 month old WT and OE hippocampi. Synaptic enrichment and fractions as detailed in B. **E**. Western blot detecting KL from WT and OE hippocampal pre-synaptic (pre) and post-synaptic (post) fractions at 2 and 6 months old. Synaptic enrichment validated as in C. (n=3–4; averaged data plotted +/− S.E.M.; T-test: *p<0.05, **p<0.005).

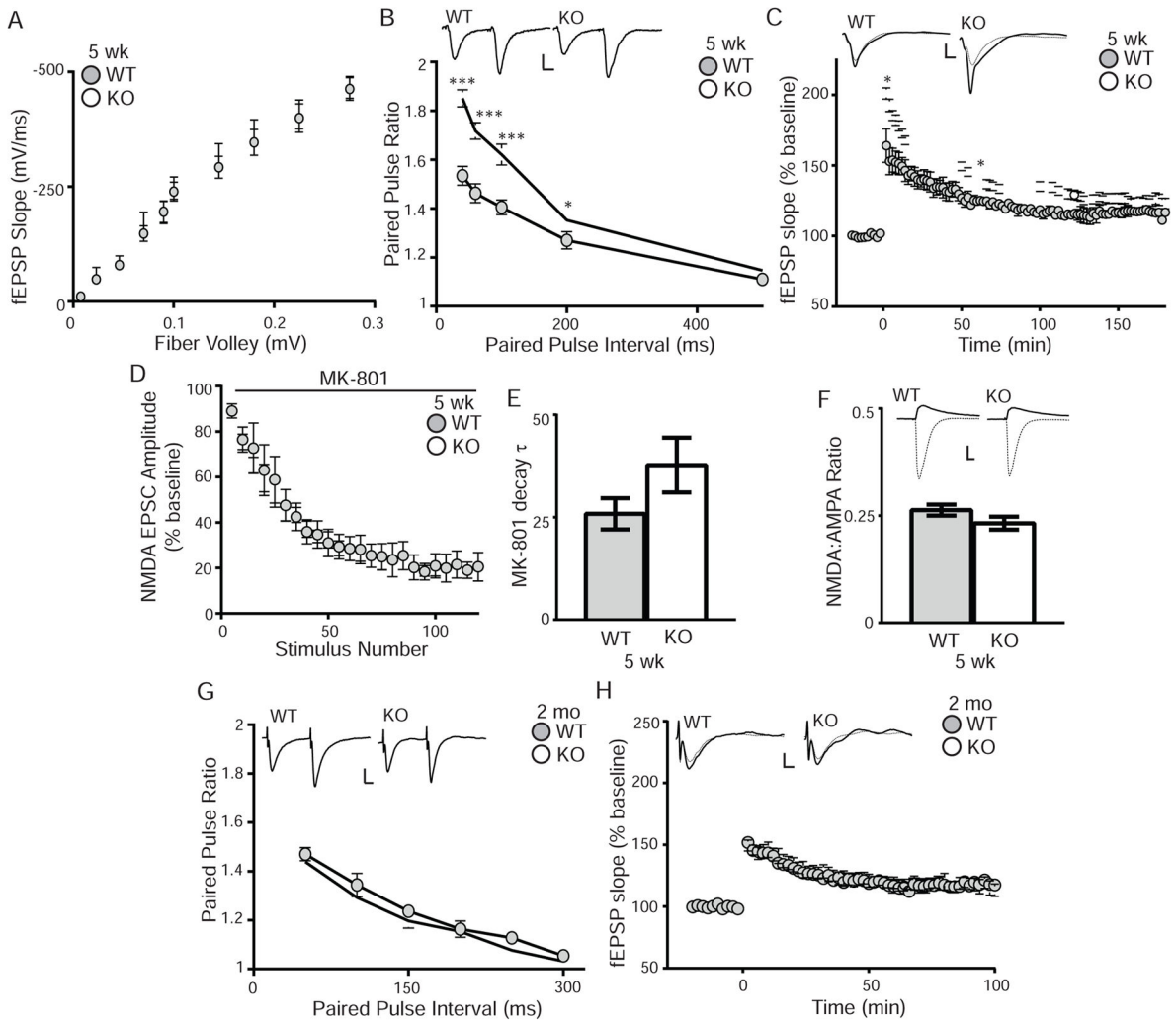

Figure 3. KL-deficiency increases paired-pulse ratio and early long-term potentiation

A. 5 week old WT and KO input-output curves plotted as the initial slopes of the evoked field EPSP (fEPSP; mVolt (mV)/mSecond (ms)) as a function of the amplitude of the fiber volley (mV). No change is measured between genotypes. **B**. 5 week old WT and KO paired-pulse ratio at 40–500 ms intervals showing enhanced PPF from KO brain slices. Traces represent the 40ms interval. Scale bar 10ms, 1mV. **C**. Enhanced KO LTP measured as the fEPSP over time before and after stimulation from 5 week old mice (5–6 mice/genotype, 2–4 slices/mouse). Representative traces represent one minute before (dashed line) and after (solid line) stimulation. Scale bar represents 5ms, 1mV. Statistical significance calculated 2 and 60 minutes after LTP induction. **D**. NMDA EPSC amplitude blocking rate by MK-801 (40μM) is not different between 5 week old WT and KO mice (5–6 mice/genotype; results displayed in 5 point bins). **E**. Decay constant (tau;**τ**) of MK801 blockade is not different between WT and KO. **F**. AMPA EPSCs (solid lines) were recorded at −70mV and NMDA EPSCs (dashed lines) were recorded at +40mV in the presence of NBQX and are not different between 5 week old WT and KO mice (6–7 animals/genotype). Graph is the ratio of NMDA to AMPA EPSC. Inset show representative traces. Scale bar is 10ms,100pA. **G**.

Paired-pulse ratio and representative traces from 7 week old WT and KO mice as in B are not difference between genotypes. **H**. No LTP change was induced in 7 week old WT and KO mice (6 mice/genotype, 4–8 slices/brain). (Averaged data plotted +/− S.E.M.; T-test: *p<0.05, ***p<0.0001).

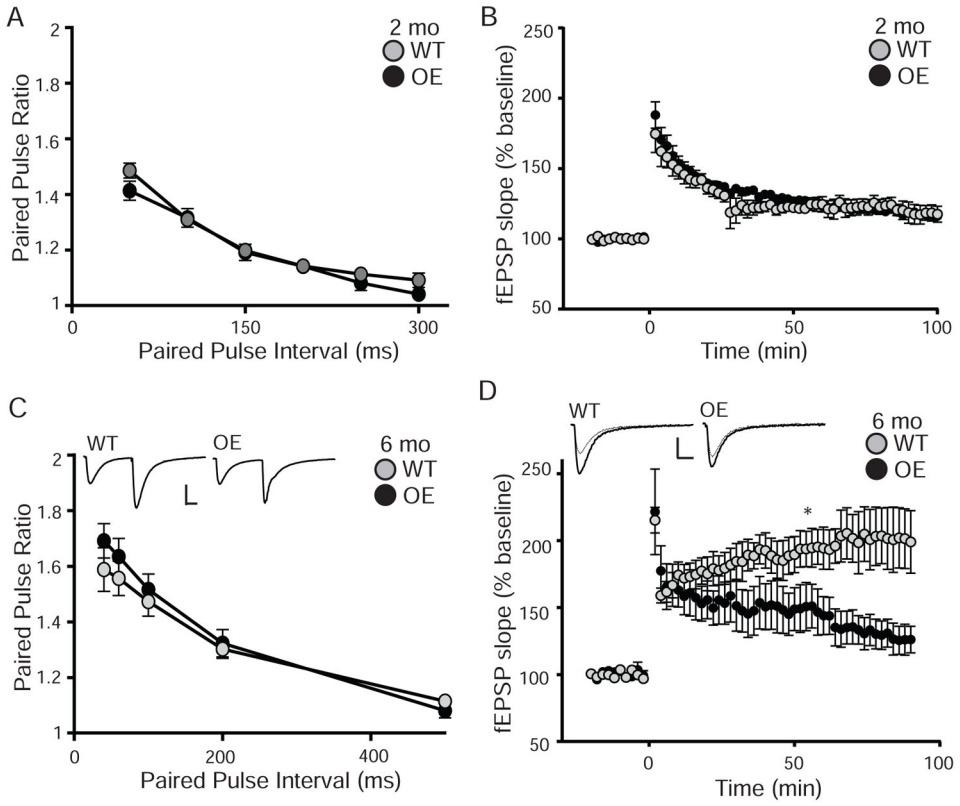

Figure 4. Overexpression of KL decreases long-term potentiation at 6 months

A. Paired-pulse ratio from 2 month old WT and OE slices at intervals from 50–300 ms (7–10 mice/genotype and 5 slices/mouse) show no difference between genotypes. **B**. LTP measured as the fEPSP over time before and after induction stimulation from 2 month old WT and OE slices (6 mice/genotype and 5 slices/mouse) also show no difference between genotypes. **C**. Paired-pulse ratio from 6 month old WT and OE slices at intervals from 40–500ms show no difference between genotypes. Traces represent the 40ms interval. Scale bar is 10ms, 0.5mV (5–6 mice/genotype, 2–4 slices/mouse). **D**. 6month old WT/OE LTP as in B show no difference between genotypes (5–6 mice/genotype, 2–4 slices/brain). Representative traces represent 1min before (dashed line) and 60min after (solid line) stimulation. Scale bar is 10ms, 0.5mV. Statistical significance calculated 60 min after LTP induction. (Averaged data plotted as +/− S.E.M.; T-test: *p<0.05).

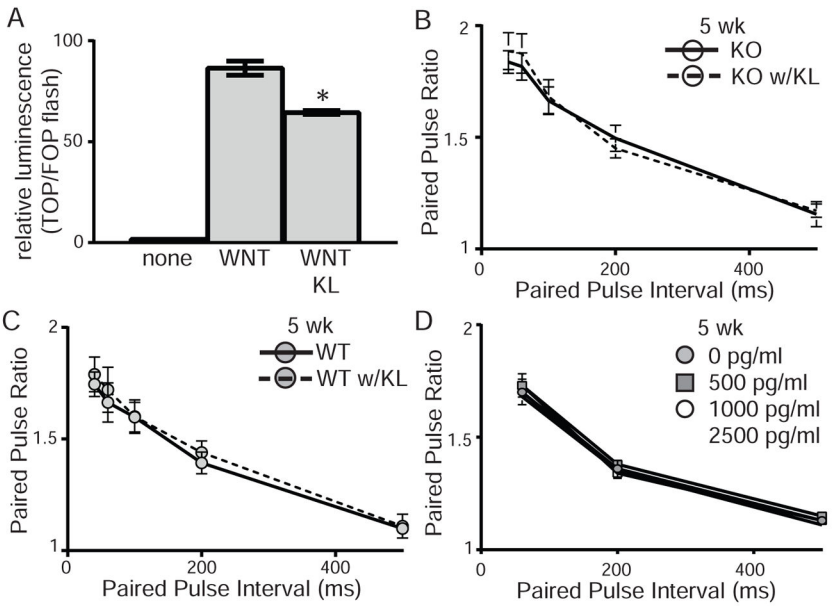

Figure 5. Acute KL application does not rescue enhanced synaptic plasticity

A. HEK 293T cells transfected with TOP or FOP-flash luciferase were incubated with no protein, recombinant wnt3a, or recombinant wnt3a and shed KL (TOP/FOP, +/− S.E.M.; t-test: *p<0.05). Addition of KL to media inhibits wnt signal transduction. **B,C.** Paired-pulse ratio from 5 week old **B.** KO or **C.** WT slices at intervals from 40–500ms. Slices were incubated with recombinant shed KL (5000pg/ml; dashed lines) or BSA (solid lines) in the ACSF before and during induction of PPF. Addition of KL to media did not affect WT or KO PPF. (n=5–6 mice/genotype, 3–4 slices/mouse; averaged data plotted +/− S.E.M.). **D.** Paired-pulse ratio from 5 week old KO slices at intervals from 60–500ms. After measuring PPF in normal ACSF (grey circle), the recombinant shed KL concentration was sequentially increased to 500 (grey square), 1,000 (white circle), and 2,500pg/ml (white square). (n=2–3 mice/genotype, 4 slices/mouse; averaged data plotted +/− S.E.M.).